

Rotating Flow of a Micropolar Fluid Induced by a Stretching Surface

Tariq Javed^a, Iftikhar Ahmad^b, Zaheer Abbas^a, and Tasawar Hayat^{c,d}

^a Department of Mathematics, FBAS, International Islamic University, Islamabad 44000, Pakistan

^b Department of Mathematics, Azad Kashmir University, Muzaffarabad 13100, Pakistan

^c Department of Mathematics, Quaid-I-Azam University 45320, Islamabad 44000, Pakistan

^d Department of Mathematics, College of Sciences, King Saud University, P. O. Box 2455, Riyadh 11451, Saudi Arabia

Reprint requests to Z. A.; Fax: +92 51 2501171; E-mail: za_qau@yahoo.com

Z. Naturforsch. **65a**, 829–836 (2010); received August 31, 2009 / revised December 16, 2009

This investigation deals with the boundary layer flow of a micropolar fluid over a stretching surface. The flow is considered in a rotating frame of reference. The governing nonlinear partial differential equations are reduced to coupled nonlinear ordinary differential equations. The set of similarity equations has been solved analytically employing the homotopy analysis method (HAM). The series solutions are given for velocity and microrotation, and the convergence of these solutions are explicitly discussed. Attention has been focused to the variations of the emerging parameters on the velocity and microrotation are discussed through graphs.

Key words: Micropolar Fluid; Stretching Sheet; Series Solution; HAM.

1. Introduction

Recent developments in engineering have led to an increasing interest in the flows of non-Newtonian fluids. Such fluids play an important role in many practical applications. The flows of these fluids have attracted the attention of engineers, mathematicians, modelers, physicists, and computer scientist in the recent past owing to their several interesting features in industry and technology. The arising equations of non-Newtonian fluids are much nonlinear, higher order, and complicated in comparison to Navier-Stokes equations. Therefore, the resulting problems pose challenges to the researchers from a different quarter. Even an intensive research work has been done on flows of the non-Newtonian fluids. A good deal of references on such flows has been presented in the recent paper of Fetecau and Fetecau [1–5], Tan and Masuoka [6, 7], Lok et al. [8, 9], Ishak et al. [10], Xu and Liao [11], and Hayat et al. [12–17].

During the last few decades tremendous progress has been made for stretching flows of viscous fluids. These analyse fluids applications in areas such as continuous coating, rolling and extrusion in manufacturing process, the boundary layer along a film in condensation process, and aerodynamic extrusion of a plastic sheet. A major interest has existed to obtain analytic solutions of the boundary layer problem of stretching

flow. The first work on this problem has been made by Sakiadis [18]. After that extensive research has been undertaken by considering more general stretching velocity applications to non-Newtonian fluids and inclusion of other physical effects such as magnetic fields, heat or mass transfer, and porous media. For non-Newtonian fluids, the model commonly used is the simplest subclass of non-Newtonian fluids, namely, the second-grade fluid. Some recent representative studies in this area may be found in the research articles by Cortell [19–21], Nazar et al. [22], and Hayat et al. [23–26]. Literature survey indicates that no attention has been given to investigate the stretching flow of a non-Newtonian fluid in a rotating frame of reference. Such analysis has promising applications in geophysics and astrophysics. Therefore, the main aim of the present investigation is to discuss the stretching rotating flow problem of a micropolar fluid. In fact the theory of micropolar fluids has been developed by Eringen [27, 28] and has received considerable interest recently. Unlike the several non-Newtonian fluids, this theory includes effects of local rotation inertia and couple stresses, and provides a mathematical model of non-Newtonian behaviour observed in certain fluids including colloidal fluids, polymeric fluids, animal blood, exotic lubricants, and real fluids with suspensions. The presence of dust or smoke particularly in a gas may also be modelled using micropolar fluid dy-

namics. The paper is divided into six sections of which this introduction is the first. The problem deformation is given in Section 2. Section 3 deals with the development of the series solution by HAM, and the convergence of the developed series solutions are given in Section 4. The analytic series solutions have been discussed through graphical representation in Section 5. Section 6 contains the concluding remarks.

2. Mathematical Formulation

Consider the steady, incompressible flow of a micropolar fluid in the region $z > 0$. We take the stretching sheet in the XOY plane. Two equal and opposite forces are applied along the x -axis. We assume that the surface is stretched in x -direction such that the x -component of the velocity varies linearly along it, i. e. $u = cx$, where c is the constant of proportionality. Both the fluid and the stretching surface are in a state of solid body rotation with constant angular velocity Ω about the z -axis. In the absence of body forces and pressure gradient, the boundary layer rotating flow of an incompressible micropolar fluid is described by the following equations:

$$\frac{\partial u}{\partial x} + \frac{\partial w}{\partial z} = 0, \quad (1)$$

$$u \frac{\partial u}{\partial x} + w \frac{\partial u}{\partial z} - 2\Omega v = \left(v + \frac{k}{\rho} \right) \frac{\partial^2 u}{\partial z^2} + \frac{k}{\rho} \frac{\partial N}{\partial z}, \quad (2)$$

$$u \frac{\partial v}{\partial x} + w \frac{\partial v}{\partial z} + 2\Omega u = \left(v + \frac{k}{\rho} \right) \frac{\partial^2 v}{\partial z^2}, \quad (3)$$

$$u \frac{\partial N}{\partial x} + w \frac{\partial N}{\partial z} = \frac{\gamma}{\rho j} \frac{\partial^2 N}{\partial z^2} - \frac{k}{\rho j} \left(2N + \frac{\partial u}{\partial z} \right). \quad (4)$$

In the above expression u , v , and w are the velocity components in x -, y -, and z -direction, respectively, N is the microrotation or angular velocity whose direction of rotation is in the xy -plane, ρ is the density, ν is the kinematic viscosity, j , γ , and k are the microinertia per unit mass, spin gradient viscosity, and vortex viscosity, respectively. Furthermore, we follow the work of many recent authors by assuming γ of the following form [29]:

$$\gamma = \left(u + \frac{k}{2} \right) j, \quad (5)$$

in which μ is the dynamic viscosity, and we take $j = \nu/cx^{\frac{1}{2}}$ as reference length. As pointed out by Ahmadi [30], relation (5) invoked (1)–(4) to predict the

correct behaviour in the limiting case when microstructure effects become negligible and microrotation N reduces to the angular velocity.

The boundary conditions of (1)–(4) are

$$u = cx, \quad v = 0, \quad w = 0, \quad N = -m_0 \frac{\partial u}{\partial z} \quad \text{at } z = 0, \quad (6)$$

$$u = 0, \quad v = 0, \quad N = 0 \quad \text{as } z \rightarrow \infty.$$

We now proceed to non-dimensionalization of the problem by introducing the variables

$$\eta = \sqrt{\frac{c}{\nu}} z, \quad N = cx \sqrt{\frac{c}{\nu}} h(\eta), \quad (7)$$

$$u = cx f'(\eta), \quad v = cx g(\eta), \quad w = -\sqrt{c\nu} f(\eta).$$

The continuity equation (1) is identically satisfied and (2)–(4) and (7) reduces to

$$(1+K)f''' + ff'' - f'^2 + 2\lambda g + Kh' = 0, \quad (8)$$

$$(1+K)g'' + fg' - f'g + 2\lambda f' = 0, \quad (9)$$

$$\left(1 + \frac{K}{2} \right) h'' + fh' - f'h + -(2h + f'') = 0, \quad (10)$$

$$f = 0, \quad f' = 1, \quad g = 0, \quad h = -m_0 f''(0) \quad \text{as } \eta = 0, \quad (11)$$

$$f' = 0, \quad g = 0, \quad h = 0 \quad \text{as } \eta \rightarrow \infty,$$

where the prime indicate differentiation with respect to η , $\lambda = \Omega/c$, and $K = k/\mu$. In the next section, we solve the nonlinear system consisting of (8)–(11) by HAM [31–38]. Recently, Liao [39] introduced an optimal homotopy-analysis approach (as three parameter optimal-HAM) for strong nonlinear differential equations. He discussed the convergence of the series solution of nonlinear differential equations by taking three auxiliary parameters $c_0 = \hbar$, c_1 , and c_2 instead of one \hbar . We use only \hbar as an auxiliary parameter and use $c_1 = c_2 = 0$ for our convenience.

3. Series Solution for $f(\eta)$, $g(\eta)$, and $h(\eta)$

Here, we have the following initial guesses and auxiliary operators:

$$f_0(\eta) = 1 - \exp(-\eta), \quad g_0(\eta) = \eta \exp(-\eta), \quad (12)$$

$$h_0(\eta) = m_0 \exp(-\eta),$$

$$L_1(f) = \frac{d^3 f}{d\eta^3} - \frac{df}{d\eta}, \quad L_2 = \frac{d^2 g}{d\eta^2} - \frac{dg}{d\eta}, \quad (13)$$

which have the properties

$$\begin{aligned} L_1[C_1 + C_2 \exp(-\eta) + C_3 \exp(\eta)] &= 0, \\ L_2[C_4 \exp(-\eta) + C_5 \exp(\eta)] &= 0 \end{aligned} \tag{14}$$

in which C_i , ($i = 1-5$) are arbitrary constants. If $p \in [0, 1]$ and h_i ($i = 1-3$) are the embedding and non-zero auxiliary parameters, respectively, then we have

i) *Zero-order deformation problem*

$$(1-p)L_1[f(\eta;p) - f_0(\eta)] = p\hbar_1 N_1[\tilde{f}(\eta;p), \tilde{g}(\eta;p), \tilde{h}(\eta;p)], \tag{15}$$

$$\tilde{f}(0;p) = 0, \quad \tilde{f}(\infty;p) = 1, \quad \tilde{f}(\infty;p) = 0, \tag{16}$$

$$(1-p)L_2[g(\eta;p) - g_0(\eta)] = p\hbar_2 N_2[\tilde{f}(\eta;p), \tilde{g}(\eta;p), \tilde{h}(\eta;p)], \tag{17}$$

$$\tilde{g}(0;p) = 0, \quad g(\infty;p) = 0, \tag{18}$$

$$(1-p)L_2[h(\eta;p) - h_0(\eta)] = p\hbar_3 N_3[\tilde{f}(\eta;p), \tilde{g}(\eta;p), \tilde{h}(\eta;p)], \tag{19}$$

$$\tilde{h}(0;p) = -m_0 f''(0;p), \quad \tilde{h}(\infty;p) = 0, \tag{20}$$

$$\begin{aligned} N_1[\tilde{f}(\eta;p), \tilde{g}(\eta;p), \tilde{h}(\eta;p)] &= \\ (1+K) \frac{\partial^3 \tilde{f}}{\partial \eta^3} + K \frac{\partial \tilde{g}}{\partial \eta} + 2\lambda \tilde{g} + \tilde{f} \frac{\partial^2 \tilde{f}}{\partial \eta^2} - \left(\frac{\partial \tilde{f}}{\partial \eta}\right)^2, \end{aligned} \tag{21}$$

$$\begin{aligned} N_2[\tilde{f}(\eta;p), \tilde{g}(\eta;p), \tilde{h}(\eta;p)] &= \\ (1+K) \frac{\partial^2 \tilde{g}}{\partial \eta^2} - \frac{\partial \tilde{f}}{\partial \eta} \tilde{g} + \tilde{f} \frac{\partial \tilde{g}}{\partial \eta} - 2\lambda \frac{\partial \tilde{f}}{\partial \eta}, \end{aligned} \tag{22}$$

$$\begin{aligned} N_3[\tilde{f}(\eta;p), \tilde{g}(\eta;p), \tilde{h}(\eta;p)] &= \\ \left(1 + \frac{K}{2}\right) \frac{\partial^2 \tilde{h}}{\partial \eta^2} - K \left(2\tilde{h} + \frac{\partial^2 \tilde{f}}{\partial \eta^2}\right) - \tilde{h} \frac{\partial \tilde{f}}{\partial \eta} + \tilde{f} \frac{\partial \tilde{h}}{\partial \eta}. \end{aligned} \tag{23}$$

Note that for $p = 0$ and $p = 1$, we have

$$\begin{aligned} \tilde{f}(\eta;0) &= f_0(\eta), \quad \tilde{f}(\eta;1) = f(\eta), \\ \tilde{g}(\eta;0) &= g_0(\eta), \quad \tilde{g}(\eta;1) = g(\eta), \\ \tilde{h}(\eta;0) &= h_0(\eta), \quad \tilde{h}(\eta;1) = h(\eta). \end{aligned} \tag{24}$$

When p increases from zero to unity $\tilde{f}(\eta;p)$, $\tilde{g}(\eta;p)$, and $\tilde{h}(\eta;p)$ vary from initial guess $f_0(\eta)$, $g_0(\eta)$, and $h_0(\eta)$ to the solutions $f(\eta)$, $g(\eta)$, and $h(\eta)$. By Taylor's theorem we can write

$$\begin{aligned} \tilde{f}(\eta;p) &= f(\eta) + \sum_{m=1}^{+\infty} f_m(\eta) p^m, \\ f_m(\eta) &= \frac{1}{m!} \frac{\partial^m \tilde{f}(\eta;p)}{\partial p^m} \Big|_{p=0}, \end{aligned} \tag{25}$$

$$\begin{aligned} \tilde{g}(\eta;p) &= g(\eta) + \sum_{m=1}^{+\infty} g_m(\eta) p^m, \\ g_m(\eta) &= \frac{1}{m!} \frac{\partial^m \tilde{g}(\eta;p)}{\partial p^m} \Big|_{p=0}, \end{aligned} \tag{26}$$

$$\begin{aligned} \tilde{h}(\eta;p) &= h(\eta) + \sum_{m=1}^{+\infty} h_m(\eta) p^m, \\ h_m(\eta) &= \frac{1}{m!} \frac{\partial^m \tilde{h}(\eta;p)}{\partial p^m} \Big|_{p=0}, \end{aligned} \tag{27}$$

where h_i ($i = 1-3$) are chosen in such a way that series are convergent at $p = 1$. Therefore, we have through (24) that

$$\begin{aligned} f(\eta) &= f_0(\eta) + \sum_{m=1}^{+\infty} f_m(\eta), \\ g(\eta) &= g_0(\eta) + \sum_{m=1}^{+\infty} g_m(\eta), \\ h(\eta) &= h_0(\eta) + \sum_{m=1}^{+\infty} h_m(\eta). \end{aligned} \tag{28}$$

ii) *The mth-order deformation problem*

$$L_1[f_m(\eta) - \chi_m f_{m-1}(\eta)] = \hbar_1 \mathcal{R}_m^f(\eta), \tag{29}$$

$$\begin{aligned} f_m(0) &= 0, \quad \frac{\partial f_m(\eta)}{\partial \eta} \Big|_{\eta=0} = 0, \\ \frac{\partial f_m(\eta)}{\partial \eta} \Big|_{\eta=+\infty} &= 0, \end{aligned} \tag{30}$$

$$L_2[g_m(\eta) - \chi_m g_{m-1}(\eta)] = \hbar_2 \mathcal{R}_m^g(\eta), \tag{31}$$

$$g_m(0) = 0, \quad g_m(\infty) = 0, \tag{32}$$

$$L_2[h_m(\eta) - \chi_m h_{m-1}(\eta)] = \hbar_3 \mathcal{R}_m^h(\eta), \tag{33}$$

$$h_m(0) - m_0 f''(0) = h_m(\infty) = 0, \tag{34}$$

$$\begin{aligned} \mathcal{R}_m^f(\eta) &= (1+K) f_{m-1}'' + K h_{m-1}' + 2\lambda g \\ &+ \sum_{k=0}^{m-1} [f_{m-1-k} f_k'' - f_{m-1-k}' f_k'], \end{aligned} \tag{35}$$

$$\begin{aligned} \mathcal{R}_m^g(\eta) &= (1+K) g_{m-1}'' - 2\lambda f' \\ &+ \sum_{k=0}^{m-1} [g_{m-1-k} f_k - g_k f_{m-1-k}'], \end{aligned} \tag{36}$$

$$\begin{aligned} \mathcal{R}_m^h(\eta) &= \left(1 + \frac{K}{2}\right) h_{m-1}'' - K(2h_{m-1} + f_{m-1}'') \\ &+ \sum_{k=0}^{m-1} [h_{m-1-k} f_k - h_k f_{m-1-k}'], \end{aligned} \tag{37}$$

$$\chi_m = \begin{cases} 0, & m \leq 1, \\ 1, & m > 1. \end{cases} \tag{38}$$

Through symbolic software Mathematica we obtain

$$f(\eta) = \sum_{n=0}^{\infty} f_n(\eta) = \lim_{M \rightarrow \infty} \sum_{m=0}^M a_{m,0}^0 \cdot \sum_{s=1}^{M+1} \exp[-s\eta] \left(\sum_{m=s-1}^M \sum_{k=0}^{m+1-s} a_{m,s}^k \eta^k \right), \tag{39}$$

$$g(\eta) = \sum_{n=0}^{\infty} g_n(\eta) = \lim_{M \rightarrow \infty} \sum_{m=0}^M b_{m,0}^0 \cdot \sum_{s=1}^{M+1} \exp[-s\eta] \left(\sum_{m=s-1}^M \sum_{k=0}^{m+1-s} b_{m,s}^k \eta^k \right), \tag{40}$$

$$h(\eta) = \sum_{n=0}^{\infty} h_n(\eta) = \lim_{M \rightarrow \infty} \sum_{m=0}^M c_{m,0}^0 \cdot \sum_{s=1}^{M+1} \exp[-s\eta] \left(\sum_{m=s-1}^M \sum_{k=0}^{m+1-s} c_{m,s}^k \eta^k \right). \tag{41}$$

4. Convergence of the Analytic Solution

The three series for the functions f , g , and h are given in (39)–(41) which contain auxiliary parameters \hbar_1 , \hbar_2 , and \hbar_3 . The convergence of these series strongly depends upon \hbar_1 , \hbar_2 , and \hbar_3 . The range for which the so-called \hbar -curve is parallel to the \hbar -axis is of admissible range. Any value of \hbar from the admissible range guarantees the convergence of the series. To see the range of admissible values of these parameters, the \hbar -curve is plotted in Figure 1 for the 15th order

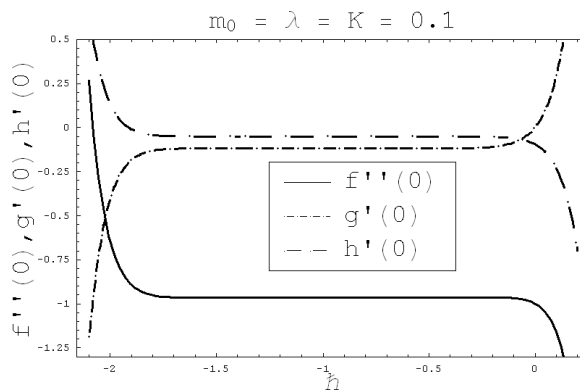


Fig. 1. \hbar -curves of $f''(0)$, $g'(0)$, and $h'(0)$ for 15th-order approximations.

of approximation for different values of the parameters involved in the series solution by taking $\hbar_1 = \hbar_2 = \hbar_3 = \hbar$. It is evident from this figure that our series solution converges for all values of $-1.6 \leq \hbar \leq -0.3$ for $m_0 = \lambda = K = 0.1$. Similarly, we can draw \hbar -curves for all other different values of the parameters involve in the equation. To see the effect of the auxiliary parameters on the series solution more closely we draw the error curves Figures 2–4 for different admissible values of the auxiliary parameter for the whole domain of the problem. It can easily be observe from Figure 2a that the error for $\eta = 0$ (solid line) and $\eta = 1$ (dash line) are less than 10^{-6} for all admissible values between $-1.4 \leq \hbar \leq -0.8$. However, it diminished to zero for $-1.3 \leq \hbar \leq -1.15$ for both $\eta = 0$ and $\eta = 1$. To see the error for the whole domain of the problem $0 \leq \eta \leq \infty$, Figure 2b is constructed. It is found that $\hbar = -1.16$ produces minimum error for the whole domain of

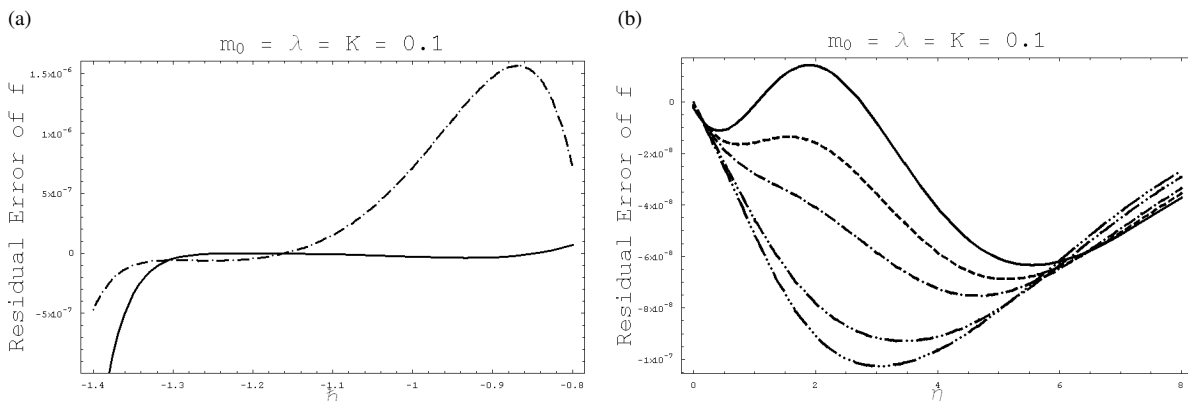


Fig. 2. (a): Error curves for f with $\eta = 0$ (solid line) and $\eta = 1$ (dash line) (b): Error curves for different values of \hbar : $\hbar = -1.16$ (solid line), $\hbar = -1.17$ (dash line), $\hbar = -1.18$ (dash-dot-dash line), $\hbar = -1.20$ (dash-dot-dot-dash line), and $\hbar = -1.21$ (dash-dot-dot-dot-dash line).

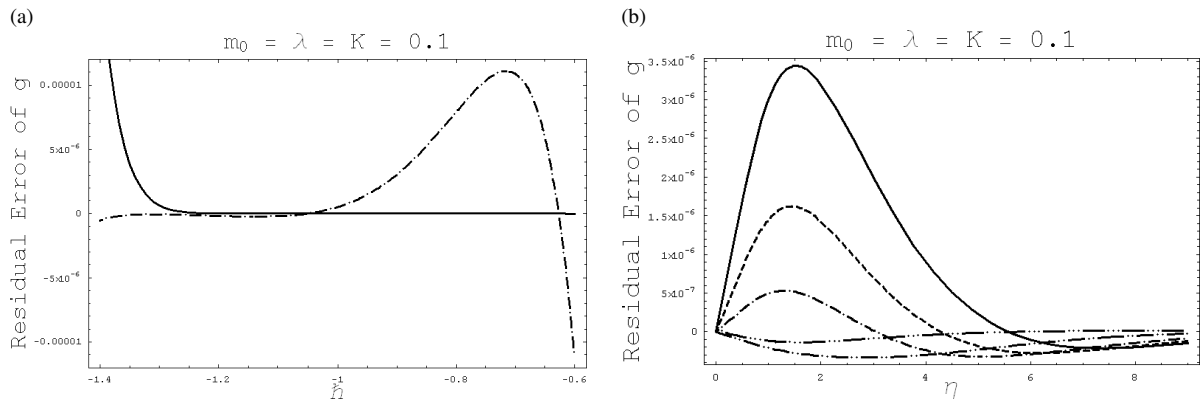


Fig. 3. (a): Error curves for g with $\eta = 0$ (solid line) and $\eta = 1$ (dash line) (b): Error curves for different values of h : $h = -1.16$ (solid line), $h = -1.17$ (dash line), $h = -1.18$ (dash-dot-dash line), $h = -1.20$ (dash-dot-dot-dash line), and $h = -1.21$ (dash-dot-dot-dot-dash line).

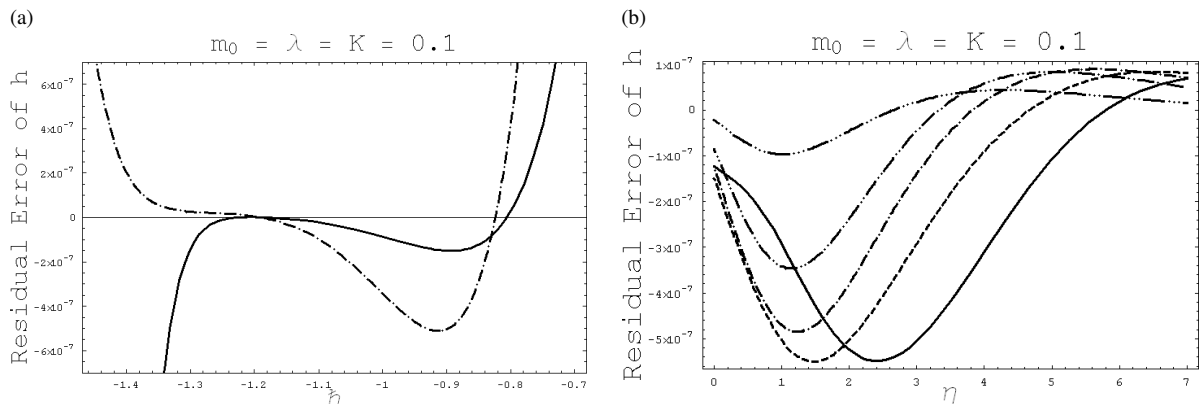


Fig. 4. (a): Error curves for h with $\eta = 0$ (solid line) and $\eta = 1$ (dash line) (b): Error curves for different values of h : $h = -1.16$ (solid line), $h = -1.17$ (dash line), $h = -1.18$ (dash-dot-dash line), $h = -1.20$ (dash-dot-dot-dash line), and $h = -1.21$ (dash-dot-dot-dot-dash line).

$0 \leq \eta \leq \infty$, and the rest of the curves for $\hat{h} = -1.17$, $\hat{h} = -1.18$, $\hat{h} = -1.20$, and $\hat{h} = -1.21$ in Figure 2b corresponds to little bigger error. This imply that $\hat{h} = -1.16$ is the best value of \hat{h} for these values of the parameters $m_0 = \lambda = K = 0.1$ for f . Similarly, to find the most appropriate values of \hat{h} for the series solution g and h which give the rapid convergence for the whole domain, Figures 3–4 are constructed. In this way we find the most appropriate values of \hat{h} for the series solution f , g , and h for all values of the parameter.

5. Result and Discussion

The system of coupled nonlinear ordinary differential equations (8)–(10) with boundary conditions (11) has been solved analytically using homotopy analysis method (HAM). Figures 5–10 are plotted to see the

effects of the involving parameters, for example, the material parameter or the vortex viscosity K , the rotation parameter λ , and the microrotation parameter m_0 on the velocity profiles f' and g and the microrotation or angular velocity h , respectively.

Figures 5–7 have been drawn in order to see the effects of the material parameter or the vortex viscosity K , the rotation parameter λ , and the microrotation parameter m_0 on the velocity components f' and g in the x - and y -axis directions, respectively. Figure 5a shows the influences of the vortex viscosity K on the velocity profile f' . It is observed that the velocity f' is an increasing function of K . The boundary layer thickness also increases for large values of the vortex viscosity K . Figure 5b elucidates the variations of the material parameter or the vortex viscosity K on the velocity component g . From this figure we can see that the

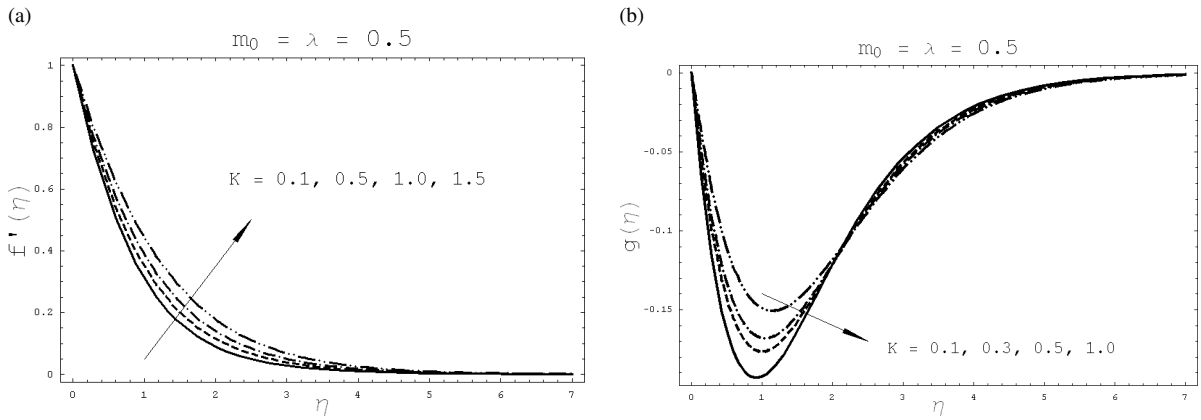


Fig. 5. Effects of the vortex-viscosity parameter K on the velocity components $f'(\eta)$ and $g(\eta)$.

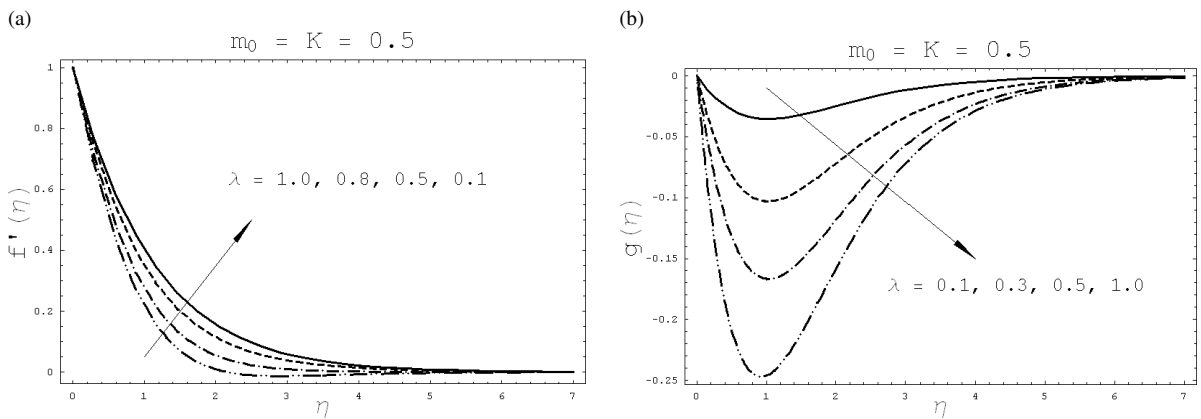


Fig. 6. Effects of the rotation parameter λ on the velocity components $f'(\eta)$ and $g(\eta)$.

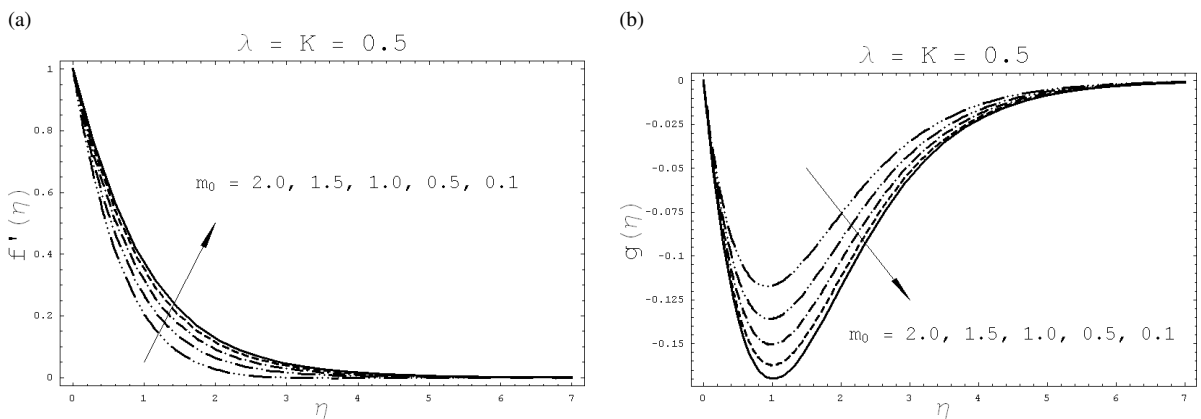


Fig. 7. Effects of the microrotation parameter m_0 on the velocity components $f'(\eta)$ and $g(\eta)$.

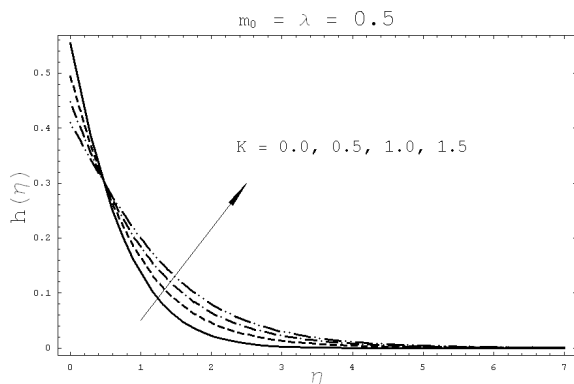


Fig. 8. Effects of the vortex-viscosity parameter K on the angular velocity h .

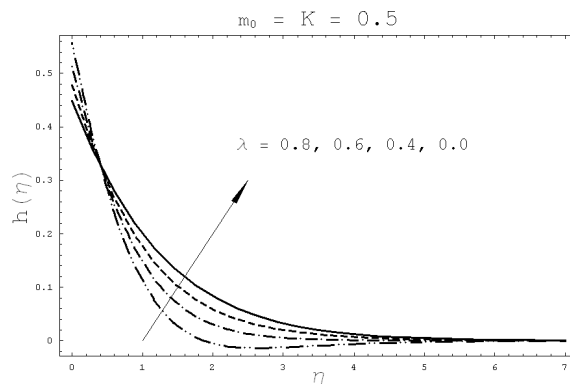


Fig. 9. Effects of the rotation parameter λ on the angular velocity h .

magnitude of the velocity g initially decreases as K increases but after $\eta = 2$, it slightly increases for higher values of K . Figure 6 depicts the influences of the rotation parameter λ on the velocity profiles f' and g . Figure 6a displays the variations of the dimensionless rotation parameter λ on the velocity f' . The velocity f' decreases when the rotation parameter λ increases. Figure 6b shows the influences of the rotation λ on the velocity profile g . It is found that the magnitude of the velocity g is an increasing function of λ . The boundary layer thickness is also decreased for large values of λ in both the cases of f' and g . Figure 7 gives the effects of m_0 on the velocity components f' and g . It is noted from Figure 7a that both the velocity f' and the boundary layer thickness are decreased as m_0 increases. Figure 7b shows the change in the velocity g for different values of m_0 . From this figure, we can say that the magnitude of g is decreased and the boundary layer thickness also decreases when m_0 increases, respectively.

Figures 8–10 are plotted to show the variations of the vortex viscosity K , the rotation parameter λ and m_0 on the microrotation or the angular velocity h . Figure 8 shows the effects of the material parameter or the vortex velocity K on the microrotation velocity h . It is noted that initially the microrotation/angular velocity h decreases but after $\eta = 0.5$, it goes to increase for large values of K . The boundary layer thickness is decreased as the vortex viscosity K increases. Figure 9 displays the variations of the rotation parameter λ on the micro-rotation velocity h . It is found that the microrotation velocity h has opposite effects for large values of λ when compared it with Figure 8. The change in the magnitude of the angular velocity h is larger in case of the rotation λ when compared with the case of

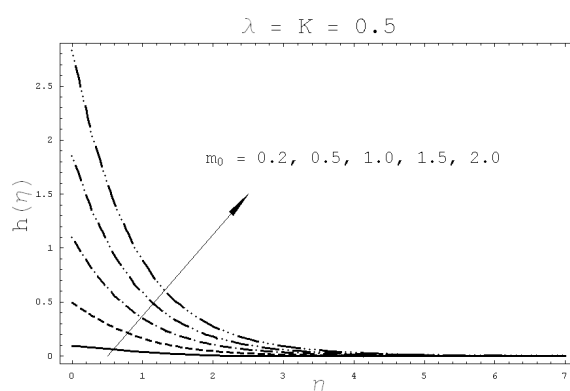


Fig. 10. Effects of the microrotation parameter m_0 on the angular velocity h .

material parameter or the vortex viscosity K . Figure 10 gives the influences of m_0 on the microrotation/angular velocity h . It is observed that the magnitude of the angular velocity h is an increasing function of m_0 . The boundary layer thickness is also increased for large values of m_0 .

6. Concluding Remarks

In the present study, the steady boundary layer flow of a micropolar fluid bounded by a stretching sheet is investigated in a rotating frame. The series solutions are developed using HAM. The convergence of these series solutions are discussed explicitly. The influence of various emerging parameters on the velocity and microrotation velocity is analyzed with the help of graphs. The value of HAM is further demonstrated as powerful and useful tool in the flow analysis of such problems. As expected, the boundary layer thickness decreases with increasing rotation parameter.

Acknowledgement

We are thankful to the referees for their values suggestions and comments to improve the version of paper.

- [1] C. Fetecau and C. Fetecau, *Int. J. Eng. Sci.* **43**, 340 (2005).
- [2] C. Fetecau and C. Fetecau, *Int. J. Eng. Sci.* **44**, 788 (2006).
- [3] C. Fetecau and C. Fetecau, *Int. J. Nonlinear Mech.* **38**, 985 (2003).
- [4] C. Fetecau and C. Fetecau, *Int. J. Nonlinear Mech.* **40**, 1214 (2005).
- [5] C. Fetecau and C. Fetecau, *Int. J. Nonlinear Mech.* **38**, 1539 (2003); **38**, 985 (2003).
- [6] W. Tan and T. Masouak, *Int. J. Nonlinear Mech.* **40**, 515 (2005).
- [7] W. Tan and T. Masouak, *Phys. Lett. A* **360**, 454 (2007).
- [8] Y. Y. Lok, P. Phang, N. Amin, and I. Pop, *Int. J. Eng. Sci.* **41**, 173 (2003).
- [9] Y. Y. Lok, N. Amin, and I. Pop, *Int. J. Therm. Sci.* **45**, 1149 (2006).
- [10] A. Ishak, R. Nazar, and I. Pop, *Commun. Nonlinear Sci. Numer. Simul.* **14**, 109 (2009).
- [11] H. Xu and S. J. Liao, *J. Non-Newtonian Fluid Mech.* **129**, 46 (2005).
- [12] T. Hayat, Z. Abbas, and M. Sajid, *Phys. Lett. A* **372**, 2400 (2008).
- [13] T. Hayat, M. Sajid, and M. Ayub, *Commun. Nonlinear Sci. Numer. Simul.* **12**, 1481 (2007).
- [14] T. Hayat, Z. Abbas, and T. Javed, *Phys. Lett. A* **42**, 637 (2008).
- [15] T. Hayat and T. Javed, *Phys. Lett. A* **370**, 243 (2007).
- [16] T. Hayat and M. Sajid, *Phys. Lett. A* **361**, 316 (2007).
- [17] T. Hayat, Z. Abbas, and M. Sajid, *Chaos, Solitons, and Fractals* **39**, 840 (2009).
- [18] B. C. Sakiadis, *AIChE J.* **7**, 26 (1961).
- [19] R. Cortell, *Int. J. Heat Mass Transfer* **49**, 1851 (2006).
- [20] R. Cortell, *Chem. Eng. Process* **46**, 721 (2007).
- [21] R. Cortell, *Int. J. Nonlinear Mech.* **29**, 155 (1994).
- [22] N. Nazar, N. Amin, and I. Pop, *Int. J. Thermal Sci.* **42**, 283 (2003).
- [23] T. Hayat, M. Khan, and M. Ayub, *Int. J. Eng. Sci.* **42**, 123 (2004).
- [24] T. Hayat, Z. Abbas, M. Sajid, and S. Asghar, *Int. J. Heat Mass Transfer* **50**, 931 (2007).
- [25] T. Hayat and Z. Abbas, *Chaos, Solitons, and Fractals* **38**, 556 (2008).
- [26] Z. Abbas, Y. Wang, T. Hayat, and M. Oberlack, *Int. J. Nonlinear Mech.* **43**, 783 (2008).
- [27] A. C. Eringen, *Int. J. Eng. Sci.* **2**, 205 (1964).
- [28] A. C. Eringen, *J. Math. Mech.* **16**, 1 (1966).
- [29] D. A. S. Rees and I. Pop, *IMA J. Appl. Math.* **61**, 179 (2001).
- [30] G. Ahmadi, *Int. J. Eng. Sci.* **14**, 639 (1976).
- [31] S. J. Liao, *Commun. Nonlinear Sci. Numer. Simul.* **11**, 326 (2006).
- [32] S. J. Liao, *Beyond perturbation: Introduction to Homotopy Analysis Method*, Chapman and Hall, Boca Raton 2003.
- [33] S. J. Liao, *Appl. Math. Comput.* **147**, 499 (2004). S. J. Liao, *J. Fluid Mech.* **385**, 101 (1999).
- [34] S. J. Liao and A. Campo, *J. Fluid Mech.* **453**, 411 (2002).
- [35] S. Abbasbandy, *Phys. Lett. A* **360**, 109 (2006).
- [36] Y. Tan and S. Abbasbandy, *Commun. Nonlinear Sci. Numer. Simul.* **13**, 539 (2008).
- [37] S. Abbasbandy and F. S. Zakaria, *Nonlinear Dyn.* **51**, 83 (2008).
- [38] S. Abbasbandy, *Int. Commun. Heat Mass Transfer* **34**, 380 (2007).
- [39] S. J. Liao, *Commun. Nonlinear Sci. Numer. Simul.* **15**, 2003 (2010).